

Monsoon rainfall and contrasting source rocks influenced sediment composition of peninsular basins along the east coast of India (western Bay of Bengal)

A. Peketi¹, A. Mazumdar¹, S.P.K. Pillutla¹, V.K.Rai², B. Sawant¹, A.V.S. Chaitanya¹, Rama krihsna¹

¹CSIR- National Institute of Oceanography, Dona Paula, Goa-403004, India

² School of Earth and Space Exploration, Arizona State University, Tempe, AZ, 85287, USA

Corresponding Author: Aditya Peketi (aditya@nio.org)

Abstract

The peninsular India is characterized by remarkable variation in lithological composition as well as contrasting rainfall distribution patterns. The erosional and weathering history of these source rocks along with monsoonal changes are archived in sediments deposited in the basins along the east of coast of India. Here, we present a 60ky record of Sr-Nd isotope ratios coupled with major elemental composition of a sediment core off Krishna-Godavari (K-G) basin, western Bay of Bengal. The marked temporal variation in $^{87}\text{Sr}/^{86}\text{Sr}$, ϵNd , and Mg/Al ratios are attributed to the changes in relative contribution of sediments from the Deccan Basalts (DcB) and Archean-Proterozoic gneissic complexes (APGC). The enhanced contribution of APGC associated with an increase in monsoon precipitation may be attributed to heightened erosion of the granitic gneissic rocks. On the other hand, a close correlation of $^{87}\text{Sr}/^{86}\text{Sr}$ ratios with Rb/Sr ratio, $\delta^{18}\text{O}_{\text{G-ruber}}$, and CIA profiles indicate the possible influence of weathering intensity on the sediment composition.

Keywords: Deccan Basalts, monsoon, provenance, weathering, peninsular India.

1. Introduction

The geochemical composition of the lithogenic components of marine sediments reflects the source rock composition (provenance) as well as weathering induced alteration caused by climatic factors (Wronkiewicz and Condie, 1987; Cullers, 1994, 1995; Derry and France-Lanord, 1996; Fralick and Kronberg, 1997; Young and Nesbitt, 1998; Wei et al., 2003, 2004; Weltje and Eynatten, 2004; Hongxia et al., 2007; Perri et al., 2012). Major, trace and rare earth elemental concentration ratios coupled with isotopic composition of Sr, Nd, Pb, Hf, etc., are commonly used to delineate the detrital sediment source compositions (Nesbitt and Young, 1982; Roser and Korsch, 1988; Lamy et al., 2000; Lim et al., 2006; Mazumdar et al., 2015; Hindshaw et al., 2018; Hu et al., 2018; Li et al., 2018; Maccali et al., 2018). Relative contributions of lithologically diverse sources towards the detrital load as well as temporal variation in the erosion (weathering) intensity controls the resultant composition of the marine sediments (Lamy et al., 2000; Awasthi et al., 2014; Miriyala et al., 2017). Rainfall intensity is one of the most important factors responsible for the erosion and subsequent transportation of sediments from the drainage basins (Subramanian, 1996; Clift et al., 2008 a, b; Zhou et al., 2017; Kuksina, 2019) to the marine depositional realms. A shift in the locus of precipitation and/or variation in the rainfall intensity in a drainage basin with contrasting lithologies would result in marked temporal variation in marine sediment composition (Lamy et al., 2000; Ahmad et al., 2005; Tripathy et al., 2011; Awasthi et al., 2014). A coupling of elemental/isotopic compositional analyses of marine sediment cores and rainfall intensity indicators (e.g., oxygen isotope ratio and sea surface salinity) may help in the reconstruction of spatio-temporal source rock contributions as well as the relation with relative variation in rainfall intensity.

Strontium ($^{87}\text{Sr}/^{86}\text{Sr}$) and Neodymium ($^{143}\text{Nd}/^{144}\text{Nd}$) isotope ratios are often used together to characterize the sediment provenance as well as the influence of weathering and erosion on the sediment composition (Colin et al., 2006; Ali et al., 2015; Miriyala et al., 2017; Hindshaw et al., 2018; Jiang et al., 2019). Unlike Sr, Nd presumably does not fractionate during chemical weathering (McCulloch and Wasserburg, 1978; Bayon et al., 2015) and is minimally affected by multiple processes such as grain size sorting and diagenesis (Goldstein and Jacobsen, 1988; McCulloch and Wasserburg, 1978; Tutken et al., 2002; Ehlert et al., 2011; Meyer et al., 2011; Garcon et al., 2014; Bayon et al., 2015). However, individual grain size fractions may show a range of Nd isotope ratios which, however, follow the same temporal trend as the bulk isotope ratios (Jonell et al., 2018). Therefore, record of Nd isotope ratios of the lithogenic fractions in a sediment core can be used as a robust proxy for understanding the temporal variation in sediment provenances (Bayon et al., 2015;

Giosan et al., 2017). Sr isotope ratio ($^{87}\text{Sr}/^{86}\text{Sr}$) of marine sediments on the other hand, responds to both differential weathering (Bain and Bacon, 1994; Clow et al., 1997; Colin et al., 2006) of Sr-bearing minerals having distinct $^{87}\text{Sr}/^{86}\text{Sr}$ ratios (Brantley et al., 1998; Bullen et al., 1997) as well as variation in the source rock composition (Franzese et al., 2009; Hu et al., 2018; Maccali et al., 2018).

Studies on Sr-Nd isotope systematics from Bay of Bengal sediments have primarily been focused on the sediment cores collected from different parts of the Bengal fan (France-Lanord et al., 1993; Colin et al., 1999; Pierson-Wickmann et al., 2001; Ahmad et al., 2005; Kessarkar et al., 2005; Galy et al., 2008, 2010; Tripathy et al., 2011; Li et al., 2018). These studies have demonstrated the relation between Sr-Nd isotopic ratios and climatic parameters like monsoon rainfall and tectonic evolution of the Himalayas. The studies show that the main fan deposits reflect the variability of detrital composition in the Ganga-Brahmaputra river system derived from the Himalayan catchments (Galy et al., 2010), whereas the eastern and western extremities of the fan show some influence on sediment derived from Andaman/Burmese region (Miriayala et al., 2017) and peninsular India (Ahmad et al., 2005; Tripathy et al., 2011) respectively.

The present study brings to light the influence of peninsular India on the Krishna-Godavari (K-G) offshore basin sediments along the east coast of India. The peninsular Indian region is characterized by a wide array of source rock compositions ranging from Cretaceous basalts to Archean-Proterozoic granitic complexes (Roy and Purohit, 2018). The region is also typified by contrasting monsoon rainfall patterns (Parthasarathy, 1984; Narkhedkar et al., 2015). These two aspects give an opportunity to establish a link between temporal variation in mineralogical/geochemical composition of the sediments deposited in the basins along the east coast of India with monsoonal variability. Major element concentrations and Sr-Nd isotope ratios of a sediment core (MD161-8; Fig. 1) from the K-G basin, off the east coast of India, is studied to reconstruct the temporal variations in sediment composition coupled with rainfall during the last 60 ky BP.

2. Geology

The K-G basin is one of the largest sedimentary basins off the east coast of peninsular India. This pericratonic rift basin lies between Kakinada in the northeast and Ongole in the southwest of Andhra Pradesh (India) and covers an area of 1,45,000 and 28,000 km² in offshore and onshore respectively (Rao, 2001; Bastia, 2007). Krishna & Godavari rivers and their tributaries are the major sediment carriers for the K-G basin. The catchment areas of Krishna and Godavari rivers are ~2,58,948 and ~3,12,812 km² respectively (Raghunath, 2006). The K-G catchment area is characterized by

contrasting source rock composition. The western part is composed of Cretaceous/Tertiary Deccan Basalts (DcB) covering ~35.3% of total catchment area whereas, the eastern part is composed of Archaean-Proterozoic graniticgneissic complex (APGC) along with charnokite/khondalite and sedimentary rocks covering ~57.5% and ~6% respectively (Biksham and Subramanian, 1988; Ramesh et al., 1989). DcB is composed mainly of minerals like pyroxene, olivine, feldspar, spinel, ilmenite, and consists of some minor mineral phases like biotite, amphibole, pseudobrookite, etc. (Melluso and Sethna, 2011). Archean cratons are mainly composed of a gneissic basement of tonalitic-trondhjemitic-granodioritic (TTG) composition, greenstone belts and K-rich granites (Windley, 1995). Most of the gneissic rocks contain quartz, plagioclase, and biotite in variable proportions along with small amounts of K-feldspar, muscovite, and hornblende (Radhakrishna and Naqvi, 1986). The granitoids consist of minerals like quartz, alkali feldspar, plagioclase and biotite. Tonalite-Trondhjemite-Granodiorites (TTG) are rich in quartz, feldspar and plagioclase. Biotite, amphiboles (e.g. hornblende), epidote, and zircon are the other accessory minerals of TTG. The weathering and erosional process of the K-G drainage basin is controlled by the south-west (SW) Indian monsoon. The rivers discharge, as well as sediment load, reaches maxima during the monsoon season (June-September) (Vaithyanathan et al., 1988; Singh, 2018). The western and the eastern parts of the drainage basins show drastically different SW monsoonal rainfall patterns (Supp. Fig. F1). The western part (DcB provenance) falls in the rain shadow of the Western Ghat ranges and receives an average annual rainfall (ANR) of 60 to 90 cm whereas the eastern part (APGC and sedimentary province) receives an ANR of 100 to 160 cm (Supp. Fig. F1). This marked difference in source rock composition (and weatherability), as well as ANR, have a far-reaching influence on the composition of riverine sediment load as well as the offshore deposits (Mazumdar et al., 2015) which show the variable contribution of DcB and APGC provenances. Particle size analyses of the riverine suspended particulate matter (SPM) shows <75 µm fraction as the dominant grain size fraction (50-53%: Biksham and Subramanian, 1988) of which montmorillonite, illite, and kaolinite contribute 76 to 85%, 2.6 to 3.2% and 1.6 to 2.6% respectively; whereas, the coarser fraction (75 to 200 µm) contributes feldspars (2.6-9.7%) and quartz (5.2-6.3%) minerals. The fine-grained fractions, as well as the montmorillonite clay, are primarily contributed by the DCB province whereas the quartz/feldspar/illite is contributed by the APGC and sedimentary provinces. Wide mineralogical and geochemical compositional variation of the sediments deposited in the shelf and slope of the K-G basin reflects the source rock compositional variation (Pattan et al., 2008; Mazumdar et al 2015). The geochemical and mineralogical studies so far indicate the absence of any contribution from the Bengal fan sedimentation on the K-G basin sediment load (Mazumdar et al., 2015).

3. Methodology

A sediment core of length 30 m (MD161-8: Lat.= 15°51.86240'N and Long.= 81° 50.06920 'E) was collected using a giant Calypso piston corer on board ORV *Marion Dufresne* (MD161). The core was recovered from the continental slope of the east coast of India at a water depth of 1033m (Fig. 1). The sediment core was collected in a PVC liner of 10 cm inner diameter. Sediment core was divided into 1 or 1.5-meter-long subsections and stored at 2°C till the laboratory analysis. Subsampling was carried out at 2 to 50 cm interval. In the present study, we have restricted all the geochemical analyses for the depth of 15.75 mbsf due to discontinuity in the age below 15.75 mbsf (Mazumdar et al., 2009). The age scale for the sediment core (MD161-8) is based on ¹⁴C dates (Mazumdar et al., 2009). ¹⁴C dates were determined using well cleaned *Globigerina ruber* and *Globigerina sacculifer* foraminifera at National Ocean Sciences AMS (NOSAMS) facility, USA.

Godavari river bed samples (from 11 locations) were collected using stainless steel Van-Veen grab sampler. Sampling locations are shown in supplementary figure F2. The Godavari river bed samples are located within the Deccan trap terrain. All the samples were freeze-dried, homogenized using agate mortar & pestle, and stored in closed containers. Sodium, Mg, Al, K, and Ca concentrations of organic carbon and inorganic carbon-free sediment fractions were determined by using an atomic absorption spectrometer (Agilent 240AA). Calibration curves were prepared by using different concentration solutions for all the metals with Sigma Aldrich standards. Chemical alteration index (CIA) was calculated by molecular proportions, from the formula: $CIA = (Al_2O_3 / (Al_2O_3 + CaO^* + Na_2O + K_2O)) * 100$, where CaO* represents Ca from silicate fraction only (Nesbitt and Young, 1982). Elemental concentrations were determined using carbonate and organic carbon-free homogenized sediments. Rubidium, Sr, and Nd concentrations were determined by Quadrupole ICP-MS (Thermo Scientific iCAP Q) using Rh as an internal standard. MAG-1 was used as a marine reference standard material for checking the accuracy and reproducibility of the analysis. The measured concentrations of the MAG-1 are within the range of the certified values. Analytical precision was monitored by multiple measurements of sample/standard, calculated RSD for all the three elements for 3 runs was less than 3%.

Sediment samples for Sr-Nd isotope ratio measurements were digested in acid cleaned Savillex PTFE containers using standard acid mixture (HF-HNO₃-HCl) recommended for dissolution of silicate rocks. Prior to silicate dissolution, carbonates in the sediment samples were removed by treating with double distilled 0.6N HCl (Pradhan et al., 2017;). Organic matter was removed by combusting the sediments at ~550°C for 4 hours. Pre-concentration of Sr and rare earth elements

(REE) was carried out following conventional cation exchange columns filled with AG50W-X8 resin. Eichrom Ln-specific resin was used to separate Nd from other REEs using 0.27N HCL as an eluent. An in-house MC-ICP-MS (NU Plasma III) was used to measure the Sr-Nd isotope ratios. Signal of the procedural blanks for both Sr and Nd were lower by three orders magnitude with respect to the samples. Hence no blank corrections were applied for Sr and Nd isotope ratios. Mass fractionation correction for Sr and Nd was applied by normalizing $^{86}\text{Sr}/^{88}\text{Sr}$ to 0.1194 and $^{146}\text{Nd}/^{144}\text{Nd}$ to 0.7219 respectively. The average $^{87}\text{Sr}/^{86}\text{Sr}$ ratio of standard SRM 987 during the analysis was 0.710247 ± 0.000021 (2σ , $n = 22$) and $^{143}\text{Nd}/^{144}\text{Nd}$ for Jndi1 standard solution was 0.512095 ± 0.000016 (2σ , $n=20$), within the recommended values. The $^{143}\text{Nd}/^{144}\text{Nd}$ values are normalized with $^{143}\text{Nd}/^{144}\text{Nd}$ ratio (0.512638) of CHUR (Chondritic Uniform Reservoir) and represented as ϵNd . The mixing curves are generated using the average Sr, Nd concentrations and isotope ratios reported from the DcB (224.34 $\mu\text{g/g}$, 21.08 $\mu\text{g/g}$, 0.707113, -3.24), APGC (377.85 $\mu\text{g/g}$, 45.66 $\mu\text{g/g}$, 0.760536, -30.72), Lower Himalayas (94 $\mu\text{g/g}$, 26 $\mu\text{g/g}$, 0.85, -24.4) and Higher Himalayas (80 $\mu\text{g/g}$, 18 $\mu\text{g/g}$, 0.76, -15). The end members for the mixing line calculation are based on data compiled from Baksi et al. (2001); Cox and Hawkesworth, (1985); Devey and Lightfoot, (1986); Harris et al. (1994); Jayananda et al. (2000); Lightfoot and Hawkesworth, (1988); Lightfoot et al. (1990); Mahoney et al. (1982, 2000); Mahoney (1988); Pandey et al. (1997); Peng et al. (1994); Peucat et al. (1989); Singh et al. (2008); Taylor et al. (1984); Vimal et al. (2012).

4. Results

The major element concentrations (Mg, Al, Ca, Na, and K), Rb, Sr, Nd concentrations and Sr-Nd isotopic ratios are presented in Table 1. Mg content varies from 1.1 to 2.2 (wt. %) whereas Al content varies between 8.2 and 12.9 (wt.%). Mg/Al ratio ranges from 0.12 to 0.18 (Avg.: 0.16) and fall in the mixing zone of DcB (Avg.: 0.5) and APGC (Avg.: 0.05) of the K-G basin catchment area (Naqvi and Rogers, 1983; Pattanayak and Shrivastava, 1999; Moyen, et al., 2003). Mg/Al ratio profile shows significant temporal variations (Fig.2B) and follows the ϵNd trend (Fig. 2A). Oxygen isotope ratio ($\delta^{18}\text{O}_{\text{G.Ruber}}$) data and demarcation of marine isotope stages (MIS I-III) in Figure 2C are from Joshi et al. (2014). Rb and Sr concentration vary from 41.9 to 251.9 and 18.3 to 154 ppm respectively. Rb/Sr ratio shows the most prominent rise (from 0.9 to 2.9) within the time window of ~16.7 ky and 1.08 ky BP and falls sharply to 2.2 within 1.08 and 0.665 ky BP (Fig. 2D). Chemical index of alteration (CIA) rises significantly (from 78.6 to 87.7) between ~16.7 ky and 0.665 ky BP (Fig.2E). Within 60 to 16.7 kyBP, the CIA shows a maximum variation of 79 to 83. $^{87}\text{Sr}/^{86}\text{Sr}$ and ϵNd values vary from 0.72477 to 0.74154 and -19.72 to -14.05 respectively. $^{87}\text{Sr}/^{86}\text{Sr}$ and ϵNd values show

overall opposite temporal trends (Fig. 2A) barring the sharp fluctuations in ϵNd observed within the time window of 22.31 to 16.15 kyBP. Lowest $^{87}\text{Sr}/^{86}\text{Sr}$ values are recorded during early MIS-III (0.72477), LGM (0.72548), and late Holocene (0.72665). $^{87}\text{Sr}/^{86}\text{Sr}$ ratio rises prominently from 0.72477 to 0.73458 and from 0.72812 to 0.73966 during the time windows of 50.54-38.6 (MIS-III) and 22.31-4.01 ky (MIS-I and II) BP respectively. These rises are superimposed by multiple perturbations over shorter time windows. Similar to the variations observed in $^{87}\text{Sr}/^{86}\text{Sr}$ ratios, ϵNd during 50.54-38.6 and 22.31-4.01 ky BP time windows drops from -16.81 to -18.53 and -14.92 to -19.72 respectively. The Sr and Nd isotopic ratios of the core MD161-8 and Godavari-Krishna river bed sediments along with the end member Sr-Nd isotopic ratios of the source rocks (DcB and APGC) are presented in Figure 3. The $^{87}\text{Sr}/^{86}\text{Sr}$ ratios and ϵNd values of the MD161-8 samples fall on or adjacent to the mixing line joining the DcB and APGC end members (Fig. 3). $^{87}\text{Sr}/^{86}\text{Sr}$ and ϵNd values of the Krishna (Ahmad et al., 2009) and Godavari (Ahmad et al., 2009 and this work) river bed samples vary from 0.70746 to 0.73006 and -18.21 to -5.32 respectively (Fig. 3; Supp. Table 1, 2). The scattering of the Sr-Nd isotope ratio across the mixing line is observed for both the sediment core and river bed sample data (Fig. 3). The clay content varies from 46.8 to 73.5 vol.% (Joshi et al., 2014). A significant rise in clay content (from 48.3 to 73.4 vol. %) is observed during the post LGM period (Fig. 4).

5. Discussion

5.1. Contrasting sediment sources: basaltic and granitic-gneissic

The ϵNd and $^{87}\text{Sr}/^{86}\text{Sr}$ ratio profiles of MD161-8 (Fig. 2A) show marked temporal variations ranging from -19.72 to -14.05 and 0.72477 to 0.74154 (Table 1) respectively and the values fall on or adjacent to the mixing line joining the DcB and APGC end members (Fig. 3). These marked temporal variations suggest variable input of both granitic and basaltic source rocks characterizing the provenance of the Krishna and Godavari river catchment areas (Fig. 1). The mixed sediment contribution by DcB and APGC end members is also evident from the river mouth bedload samples showing intermediate Nd and Sr isotope ratios ($^{87}\text{Sr}/^{86}\text{Sr}$: 0.71963 to 0.73006; ϵNd : -18.22 to -12.04; Fig. 3; Supp. Table 1), whereas samples from the higher reaches (Supp. Fig. F2) of the Godavari catchment ($^{87}\text{Sr}/^{86}\text{Sr}$: 0.70746 to 0.71682; ϵNd : -11.59 to -5.32; Fig. 3; Supp. Table 2) free from the influence of granitic terrain fall closer to the DcB end-member composition. The bulk sediment Sr-Nd isotope ratios are primarily controlled by the fluvial flux since the contribution of aeolian dust input is likely to be insignificant in the study area (Goldberg and Griffin, 1970; Mahowald et al.,

2006). An end-member mixing calculation using ϵNd values following Faure and Mensing, (2009) shows DcB contribution ranging from 59.1 to 76.9% (Fig. 3). The relatively higher contribution of DcB is also evident from the dominance of smectite ($60\pm 7.3\%$) relative to illite ($14.6\pm 2.9\%$) and kaolinite+chlorite ($25.3\pm 5\%$) clay minerals in MD161-8 (Peketi, 2013). Smectite formation is commonly attributed to the weathering of basalts, whereas, weathering of granitic sources result in the formation of illite or kaolinite minerals (Essington, 2004). Clay mineralogical composition of the Godavari river bed sediments also shows higher content of smectite ($73.6\pm 5.1\%$) compared to illite ($12\pm 2.6\%$) and kaolinite+chlorite ($14.3\pm 3.5\%$) supporting the predominance of DcB contribution to the K-G basin sediments (Naidu et al., 1985; Rao, 1991). The relatively higher contribution of the DcB to the K-G basin sediment load may be attributed to the significantly greater weatherability of basalt compared to the granitic-gneissic rocks (Dessert et al., 2003; Ibarra et al., 2016) owing to the low stability of the fine-grained ferromagnesian mineralogy of the basalt rocks contrast to the stable coarse-grained quartzo-feldspathic mineralogy of the granitic rocks. The dual input of detritus flux (Mazumdar et al., 2015) from DcB and APGC is further corroborated by Mg/Al (0.12 to 0.18; Fig. 2B) ratio profile that follows ϵNd trend (Fig. 2A) and fall between the Mg/Al ratios of DcB (Average $(\text{Mg}/\text{Al})_{\text{APGC}}$: 0.5; Pattanyak and Shrivastava, 1999) and APGC (Average $(\text{Mg}/\text{Al})_{\text{APGC}}$: 0.05; Naqvi and Rogers, 1983). Higher Mg/Al ratio of DcB over APGC is because of ferromagnesian mineralogy of the DcB. This contrasting Mg/Al ratios of the DcB and APGC can be used as a geochemical tool to understand the sediment contribution by individual sediment sources. Sediment provenance study based on Mg/Al was earlier reported by Lim et al. (2006) from the Yellow sea to differentiate the sediments into different groups. Similarly, Amorosi et al, (2007) reported enhanced sediment contribution by eastern Alpine in the marine sediments based on the Mg/Al ratios. Our results reveal lack of significant sediment contribution from the Himalayan sources such as Trans-Himalayan batholiths, Tethyan sedimentary series, Lesser Himalayas and High Himalayan Crystalline Sequence (Galy and France-Lanord, 2001; Wasson, 2003; Singh et al., 2007) which may be attributed to shallower (1033 mbsl) core location. On the other hand, sediments from the deepwater core locations (~3003: Tripathy et al., 2011) from the Bengal fan reveals significant sediment contribution from Himalayan sources. The Sr-Nd isotopic compositions of the sediment core SK187/PC33 fall far from the data of the present study and close to the Himalayan sediment sources (Fig. 3).

5.2. Past variation in the sediment sources: influence of monsoonal rainfall

The ϵNd values and $^{87}\text{Sr}/^{86}\text{Sr}$ ratios show marked temporal variation in the last 60 ky BP (Fig. 2A). This time span covers three marine isotope stages (MIS-I to MIS-III) characterized by distinct marine oxygen isotopic signals, where MIS-I, MIS-II, and MIS-III represent interglacial, glacial and interstadial time periods respectively (Past Interglacials Working Group of PAGES, 2016). In this study, we have used the $\delta^{18}\text{O}$ values of the surface-dwelling foraminifera (*Globigerinoides ruber*) of the core MD161-8 (Joshi et al., 2014) as an indicator of monsoonal precipitation and fluvial inputs since the change in SST is minor ($\sim 2^\circ\text{C}$) in the Bay of Bengal across the glacial-interglacials (Kudrass et al., 2001; Sijinkumar et al., 2016). In the Indian subcontinent, monsoonal rainfall is the key factor controlling erosion and weathering of the source region (Clift et al., 2008a; Clift et al., 2014). The temporal variation of Nd and Sr isotope ratios (Fig. 2A) are correlated with the $\delta^{18}\text{O}_{G.ruber}$ to address the link between monsoonal rainfall variability with the relative contribution of DcB and APGC provenances. The correlation between ϵNd with $\delta^{18}\text{O}_{G.ruber}$ profile (Figure 2) shows a rise in relative contribution from APGC with an increase in monsoon intensity and vice versa. Enhancement of granitic contribution with monsoonal strengthening (lowering of $\delta^{18}\text{O}_{G.ruber}$ values in Fig. 2C) is most prominent during the post LGM period (~ 20 to 5 ky BP) where the ϵNd values shift from -14.9 to -19.7 and $^{87}\text{Sr}/^{86}\text{Sr}$ from 0.72548 to 0.74010. Enhanced contribution of APGC terrain during monsoon strengthening is also evident from the mineral magnetic studies (Kulkarni et al., 2015) in sediment cores of K-G basin which show reduced ferrimagnetic signal during stronger monsoon owing to an enhanced contribution of dia and paramagnetic minerals (hematite) derived from the APGC terrain. The late Holocene (< 4 ky), characterized by marked drop in monsoonal rainfall (aridification) evident from paleo-salinity (Kudras et al., 2001; Rashid et al., 2011) and $\delta^{13}\text{C}_{\text{TOC}}$ records (Ponton et al., 2012; Joshi et al., 2014) is associated with an increase in ϵNd values (from -19.7 to -14) and decrease in $^{87}\text{Sr}/^{86}\text{Sr}$ ratios. This is attributed to the relative increase in sediment contribution by DcB. Prior to the late Holocene (< 4 ky), a spike in ϵNd and $^{87}\text{Sr}/^{86}\text{Sr}$ during the 5.2-4.01 ky time window indicate an increase in relative contribution from DcB, which is also supported by sharp rise in Mg/Al (0.12 to 0.16) ratios (Fig. 2B). This spike may be attributed to an abrupt aridity event during 4 to 5 ky span. The abrupt weakening of monsoon during this short period has also been reported from NE India, Tibetan plateau (Hong et al 2003; Berkelhammer et al., 2012), western (Dixit et al., 2014) and central (Prasad et al., 2014) Indian regions. During MIS-II, the ϵNd and $^{87}\text{Sr}/^{86}\text{Sr}$ show marked fluctuation from -17.9 to -14.9 and 0.72548 to 0.73358. The 14.6 to 20.19 kyBP time window is characterized by a zone of relatively high radiogenic Nd and less radiogenic Sr

suggesting consistently enhanced contribution from the DcB provenance. The enriched $\delta^{18}\text{O}_{G-ruber}$ values during this time window suggest significant weakening of SW monsoon rainfall (Kudrass et al., 2001; Govil and Naidu, 2010; Silva et al., 2017). Although enhancement of winter (NE) monsoon has been reported during LGM (Duplessy, 1982; Tiwari et al., 2005; Ahmad et al., 2008), similar ^{18}O depletion is not observed in Kudrass et al. (2001) and in our studied core (Joshi et al., 2014). The systematic decrease in ϵNd values from -16.6 to -18.7 and increase in $^{87}\text{Sr}/^{86}\text{Sr}$ ratios from 0.72477 to 0.73414 coupled with decrease in Mg/Al observed within the broad time window from ~52 to 39 ky BP (Fig. 2, in the MIS-III), suggest an increase in the APGC input. Our $\delta^{18}\text{O}_{G-ruber}$ data suggest a rise in summer monsoon rainfall during this time interval. Strengthening of SW monsoon rainfall during MIS-III is also evident from Ahmad et al. (2008); Govil and Naidu, (2010) and Silva et al. (2017). The observed relation between enhanced monsoonal precipitation and an increase in APGC contribution may be attributed to greater physical erosion of the APGC terrain with higher precipitation (Kulkarni et al., 2015). Enhanced monsoonal discharge leads to greater erodibility and reduced transportation time from source to sink (Clift et al., 2019). Depletion in monsoonal rainfall would result in a diminished contribution from APGC terrain, however, owing to much greater weatherability of basalt, DcB would remain a significant detrital sediment source (primarily clay minerals). Our results show the geochemical/mineralogical sediment composition (relative sediment contribution by DcB and APGC) is predominantly controlled by monsoon strength variability. In this geological framework, we propose a hypothesis that, reconstruction of paleomonsoon variability can be carried out based on temporal variation in the geochemical/mineralogical composition of sediment with contrasting sediment sources.

The profiles of $^{87}\text{Sr}/^{86}\text{Sr}$ ratio and ϵNd show good correlation suggesting a pronounced influence of source rock composition on the $^{87}\text{Sr}/^{86}\text{Sr}$ ratios as well. However, $^{87}\text{Sr}/^{86}\text{Sr}$ ratios are also known to be influenced by chemical weathering intensity at the provenance (Bain and Bacon, 1994; Bullen et al., 1997; Brantley et al., 1998) which in turn is primarily controlled by monsoonal rainfall (Hu et al., 2018; Clift et al., 2019) as well as the grain size distribution of the sediments (Meyer et al., 2011). A rise in $^{87}\text{Sr}/^{86}\text{Sr}$ ratios with enhanced clay contents (Meyer et al., 2011) has earlier been attributed to enrichment of radiogenic Sr in the clay minerals derived from Rb bearing mineral phases such as K-feldspar (Brass, 1975; Blum and Erel, 1997; Meyer et al., 2011). However, our results do not show a good covariance of the $^{87}\text{Sr}/^{86}\text{Sr}$ ratios and clay content (Fig. 4), except during the post LGM period (20 to 8 ky BP). The rise in $^{87}\text{Sr}/^{86}\text{Sr}$ ratios during the post LGM period was attributed to enhanced granitic contribution with monsoonal

enhancement(section 5.2).Thus it is difficult to decouple the role of relative rise in clay content and enhanced granitic contribution on increase in $^{87}\text{Sr}/^{86}\text{Sr}$ ratios during the post LGM period.The clay content and $^{87}\text{Sr}/^{86}\text{Sr}$ ratios profiles show opposite correlation within ~0 to 8 ky BP indicate the lack of influence of clay on the $^{87}\text{Sr}/^{86}\text{Sr}$ ratios in this time period.

The covariance of CIA,Rb/Sr ratios and $\delta^{18}\text{O}$ with $^{87}\text{Sr}/^{86}\text{Sr}$ ratios through last 60 ky (Fig. 2) suggest a possible influence of climatic changes like monsoonal intensity on the weathering of source rocks(Derry and France-Lanord, 1996; Chen et al., 1999; Hu et al., 2018).Differential dissolution kinetics of different Sr bearing minerals like Ca-plagioclase feldspar, K-Feldspar, and Biotite,etc., in the weathered rocks is commonly attributed as one of the major reasonsfor the variation in the Sr isotope ratios of the residual products which are eroded and transported to the depocenters (Brass, 1975; Bullen et al., 1997; Wei et al., 2018). The differential dissolution of mineral phases like calcite, apatite, biotite, feldspars, etc., and its influence on the $^{87}\text{Sr}/^{86}\text{Sr}$ ratios of the effluent solution/solid phases have been experimentally demonstrated by Brantley et al. (1998), Erel et al. (2004). Erel et al. (2004) showedpredominant dissolution of trace phases like calcite/apatites during the initial stages of granitoid weathering,which is followed by the dissolution of mineral phases like biotites and plagioclase during the intermediate and late weathering stages respectively. Brantley et al. (1998) reported a transient non-stoichiometric release of Srduring the initial phase (1000 to ~2500 hours) of the dissolution of different feldspars. However, in the late stage of dissolution,the $^{87}\text{Sr}/^{86}\text{Sr}$ ratios of the effluent and the residual solid phase merges. Field studies by Bullen et al. (1997) show a systematic drop in the $^{87}\text{Sr}/^{86}\text{Sr}$ ratios of the exchangeable pool with soil age which is attributed to faster weathering of biotites(more radiogenic)overplagioclase (Bullen et al., 1997). The overall correlation between CIA,Rb/Sr and $^{87}\text{Sr}/^{86}\text{Sr}$ (Fig. 2) suggests the probable influence of weathering intensity on thesediment deposition.Hence in the present study,we attribute the close relation between Rb/Sr, CIA, $^{87}\text{Sr}/^{86}\text{Sr}$ to the combined influence of provenance as well as the variable weathering intensity induced by monsoon intensity variations.

6. Conclusion

The present study from the K-G basin reveals the coupled influence of temporal variation in monsoonal rainfall and contrasting source rock compositions (DcB and APGC) on geochemical/mineralogical makeup of the sediments deposited along the east coast of peninsular India.The marked temporal variation in ϵNd , $^{87}\text{Sr}/^{86}\text{Sr}$, and Mg/Al concentration ratios reveal variable DcB and APGC contributions to the K-G basin sedimentation during the last 60 ky BP.The relatively higher contribution of the DcB over APGC may be attributed to the significantly greater

weatherability of basalt compared to the granitic-gneissic rocks. Higher contribution by APGC associated with higher monsoon is attributed to heightened erosion of the granitic gneissic rocks. Our results also reveal the lack of significant sediment contribution from Himalayan sources to the K-G basin sediments. The possible influence of weathering of the source rock on $^{87}\text{Sr}/^{86}\text{Sr}$ ratios of K-G basin sediments is revealed by the correlation of $^{87}\text{Sr}/^{86}\text{Sr}$ ratios with Rb/Sr, CIA and $\delta^{18}\text{O}_{G-ruber}$ data. We emphasize here that detailed investigation of sediment cores from other peninsular basins along the east coast of India could reveal much-needed information on the erosion-weathering history of peninsular India through glacial-interglacial cycles.

Acknowledgments

We thank the directors of NIO, PRL, NIOT, NCPOR, advisor MOES, for supporting this study. Head oceanography department and in-charge on-board operations of IPEV are thanked for providing onboard technical support and facilities. Sincere thanks to students of Goa University, IIT Kharagpur, and project scientists of NIO, NIOT, PRL, and NGRI. Thanks are due to G. Prabhu for carrying out XRD analyses. The complete data set is included in the manuscript as supplementary tables. We will upload the data at the relevant site once the manuscript is accepted.

References:

- Ahmad, S.M., Babu, G.A., Padmakumari, V.M., Dayal, A.M., Sukhija, B.S., Nagabhushanam, P., 2005. Sr, Nd isotopic evidence of terrigenous flux variations in the Bay of Bengal: Implications of monsoons during the last ~34,000 years. *Geophysical Research Letters* 32, L22711.
- Ahmad, S.M., Babu, G.A., Padmakumari, V.M., Raza, W., 2008. Surface and deep water changes in the northeast Indian Ocean during the last 60 ka inferred from carbon and oxygen isotopes of planktonic and benthic foraminifera. *Palaeogeography, Palaeoclimatology, Palaeoecology* 262, 182-188.
- Ahmad, S.M., Padmakumari, V.M., Babu, G.A., 2009. Strontium and neodymium isotopic compositions in sediments from Godavari, Krishna and Pennar rivers. *Current science* 97, 1766-1769.
- Ali, S., Hathorne, E.C., Frank, M., Gebregiorgis, D., Statterger, K., Stumpf, R., Kutterolf, S., Johnson, J.E., Giosan, L., 2015. South Asian monsoon history over the past 60 kyr recorded by radiogenic isotopes and clay mineral assemblages in the Andaman Sea. *Geochemistry, Geophysics, Geosystems* 16, 505-521.
- Amorosi, A., Colalongo, M.L., Dinelli, E., Lucchini, F., Vaiani, S.C., 2007. Cyclic variations in sediment provenance from late Pleistocene deposits of the eastern Po Plain, Italy. *SPECIAL PAPERS-GEOLOGICAL SOCIETY OF AMERICA* 420, 13.
- Awasthi, N., Ray, J.S., Singh, A.K., Band, S.T., Rai, V.K., 2014. Provenance of the Late Quaternary sediments in the Andaman Sea: Implications for monsoon variability and ocean circulation. *Geochemistry, Geophysics, Geosystems* 15, 3890-3906.
- Bain, D.C., Bacon, J.R., 1994. Strontium isotopes as indicators of mineral weathering in catchments. *Catena* 22, 201-214.
- Baksi, A.K., 2001. The Rajahmundry Traps, Andhra Pradesh: Evaluation of their petrogenesis relative to the Deccan Traps. *Proc. Indian Acad. Sci. (Earth Planet. Sci.)* 110, 397-407.
- Bastia, R., 2007. *Geologic Settings and Petroleum Systems of India's East Coast Offshore Basins: Concepts and Applications*. TECHNOLOGY PUBLICATIONS.
- Bayon, G., Toucanne, S., Skonieczny, C., Andre, L., Bermell, S., Cheron, S., Dennielou, B., Etoubleau, J., Freslon, N., Gauchery, T., 2015. Rare earth elements and neodymium isotopes in world river sediments revisited. *Geochimica et Cosmochimica Acta* 170, 17-38.
- Berkelhammer, M., Sinha, A., Stott, L., Cheng, H., Pausata, F.S.R., Yoshimura, K., 2012. An abrupt shift in the Indian monsoon 4000 years ago. *Geophys. Monogr. Ser* 198, 75-87.
- Biksham, G., Subramanian, V., 1988. Sediment transport of the Godavari River basin and its controlling factors. *Journal of Hydrology* 101, 275-290.
- Blum, J.D., Erel, Y., 1997. Rb-Sr isotope systematics of a granitic soil chronosequence: The importance of biotite weathering. *Geochimica et Cosmochimica Acta* 61, 3193-3204.

- Brantley, S.L., Chesley, J.T., Stillings, L.L., 1998. Isotopic ratios and release rates of strontium measured from weathering feldspars. *Geochimica et Cosmochimica Acta* 62, 1493-1500.
- Brass, G.W., 1975. The effect of weathering on the distribution of strontium isotopes in weathering profiles. *Geochimica et Cosmochimica Acta* 39, 1647-1653.
- Bullen, T., White, A., Blum, A., Harden, J., Schulz, M., 1997. Chemical weathering of a soil chronosequence on granitoid alluvium: II. Mineralogic and isotopic constraints on the behavior of strontium. *Geochimica et Cosmochimica Acta* 61, 291-306.
- Chen, J., An, Z., Head, J., 1999. Variation of Rb/Sr ratios in the loess-paleosol sequences of central China during the last 130,000 years and their implications for monsoon paleoclimatology. *Quaternary Research* 51, 215-219.
- Clift, P.D., Giosan, L., Blusztajn, J., Campbell, I.H., Allen, C., Pringle, M., Tabrez, A.R., Danish, M., Rabbani, M.M., Alizai, A., 2008a. Holocene erosion of the Lesser Himalaya triggered by intensified summer monsoon. *Geology* 36, 79-82.
- Clift, P.D., Hodges, K., Heslop, D., Hannigan, R., Hoang, L.V., Calves, G., 2008b. Greater Himalayan exhumation triggered by Early Miocene monsoon intensification. *Nature Geoscience* 1, 875-880.
- Clift, P.D., Wan, S., Blusztajn, J., 2014. Reconstructing chemical weathering, physical erosion and monsoon intensity since 25Ma in the northern South China Sea: A review of competing proxies. *Earth-Science Reviews* 130, 86-102.
- Clift, P.D., Kulhanek, D.K., Zhou, P., Bowen, M.G., Vincent, S.M., Lyle, M., Hahn, A., 2019. Chemical weathering and erosion responses to changing monsoon climate in the Late Miocene of Southwest Asia. *Geological Magazine*, 1-17.
- Clow, D.W., Mast, M.A., Bullen, T.D., Turk, J.T., 1997. Strontium 87/strontium 86 as a tracer of mineral weathering reactions and calcium sources in an alpine/subalpine watershed, Loch Vale, Colorado. *Water Resources Research* 33, 1335-1351.
- Colin, C., Turpin, L., Bertaux, J., Desprairies, A., Kissel, C., 1999. Erosional history of the Himalayan and Burman ranges during the last two glacial-interglacial cycles. *Earth and Planetary Science Letters* 171, 647-660.
- Colin, C., Turpin, L., Blamart, D., Frank, N., Kissel, C., Duchamp, S., 2006. Evolution of weathering patterns in the Indo-Burman Ranges over the last 280 kyr: Effects of sediment provenance on $^{87}\text{Sr}/^{86}\text{Sr}$ ratios tracer. *Geochemistry, Geophysics, Geosystems* 7.
- Cox, K., Hawkesworth, C., 1985. Geochemical stratigraphy of the Deccan Traps at Mahabaleshwar, Western Ghats, India, with implications for open system magmatic processes. *Journal of Petrology* 26, 355-377.
- Cullers, R.L., 1994. The controls on the major and trace element variation of shales, siltstones, and sandstones of Pennsylvanian-Permian age from uplifted continental blocks in Colorado to platform sediment in Kansas, USA. *Geochimica et Cosmochimica Acta* 58, 4955-4972.

- Cullers, R.L., 1995. The controls on the major-and trace-element evolution of shales, siltstones and sandstones of Ordovician to Tertiary age in the Wet Mountains region, Colorado, USA. *Chemical Geology* 123, 107-131.
- Derry, L.A., France-Lanord, C., 1996. Neogene Himalayan weathering history and river $^{87}\text{Sr}/^{86}\text{Sr}$: impact on the marine Sr record. *Earth and Planetary Science Letters* 142, 59-74.
- Dessert, C., Dupre, B., Gaillardet, J., Francois, L.M., Allegre, C.J., 2003. Basalt weathering laws and the impact of basalt weathering on the global carbon cycle. *Chemical geology* 202, 257-273.
- Devey, C.W., Lightfoot, P.C., 1986. Volcanological and tectonic control of stratigraphy and structure in the western Deccan Traps. *Bulletin of volcanology* 48, 195-207.
- Dixit, Y., Hodell, D.A., Petrie, C.A., 2014. Abrupt weakening of the summer monsoon in northwest India~ 4100 yr ago. *Geology* 42, 339-342.
- Duplessy, J., 1982. Glacial to interglacial contrasts in the northern Indian Ocean. *Nature* 295, 494-498.
- Ehlert, C., Frank, M., Haley, B.A., Boniger, U., De Deckker, P., Gingele, F.X., 2011. Current transport versus continental inputs in the eastern Indian Ocean: Radiogenic isotope signatures of clay size sediments. *Geochemistry, Geophysics, Geosystems* 12.
- Erel, Joel D. Blum, Emmanuelle Roueff, Ganor, J., 2004. Lead and strontium isotopes as monitors of experimental granitoid mineral dissolution. *Geochimica et Cosmochimica Acta* 68, 4649-4663.
- Essington, M.E., 2004. *Soil and water chemistry, An integrative approach*. CRC Press LLC. Boca Raton, 534.
- Faure, G., Mensing, T.M., 2009. *Isotopes: Principles and Applications*. Wiley, p. 897.
- Franzese, A.M., Hemming, S.R., Goldstein, S.L., 2009. Use of strontium isotopes in detrital sediments to constrain the glacial position of the Agulhas Retroflexion. *Paleoceanography* 24.
- Fralick, P.W., Kronberg, B.I., 1997. Geochemical discrimination of clastic sedimentary rock sources. *Sedimentary Geology* 113, 111-124.
- France-Lanord, C., Derry, L., Michard, A., 1993. Evolution of the Himalaya since Miocene time: isotopic and sedimentological evidence from the Bengal Fan. *Geological Society, London, Special Publications* 74, 603-621.
- Galy, A., France-Lanord, C., 2001. Higher erosion rates in the Himalaya: Geochemical constraints on riverine fluxes. *Geology* 29, 23-26.
- Galy, V., François, L., France-Lanord, C., Faure, P., Kudrass, H., Palhol, F., Singh, S.K., 2008. C4 plants decline in the Himalayan basin since the Last Glacial Maximum. *Quaternary Science Reviews* 27, 1396-1409.

- Galy, V., France-Lanord, C., Peucker-Ehrenbrink, B., Huyghe, P., 2010. Sr-Nd-Os evidence for a stable erosion regime in the Himalaya during the past 12 Myr. *Earth and Planetary Science Letters* 290, 474-480.
- Garcon, M., Chauvel, C., France-Lanord, C., Limonta, M., Garzanti, E., 2014. Which minerals control the Nd-Hf-Sr-Pb isotopic compositions of river sediments? *Chemical Geology* 364, 42-55.
- Giosan, L.P., Camilo; Usman, Muhammed; Blusztajn, Jerzy; Fuller, Dorian Q.; Galy, Valier; Haghypour, Negar; Johnson, Joel E.; McIntyre, Cameron; Wacker, Lukas, 2017. Massive erosion in monsoonal central India linked to late Holocene land cover degradation. *Earth Surface Dynamics* 5, 781-789.
- Goldberg, E.D., Griffin, J.J., 1970. The sediments of the northern Indian Ocean, *Deep Sea Research and Oceanographic Abstracts*. Elsevier, pp. 513-537.
- Goldstein, S.J., Jacobsen, S.B., 1988. Nd and Sr isotopic systematics of river water suspended material: implications for crustal evolution. *Earth and Planetary Science Letters* 87, 249-265.
- Govil, P., Naidu, P.D., 2010. Evaporation-precipitation changes in the eastern Arabian Sea for the last 68 ka: Implications on monsoon variability. *Paleoceanography* 25, 11.
- Harris, N.B.W., Santosh, M., Taylor, P.N., 1994. Crustal evolution in South India: constraints from Nd isotopes. *The Journal of Geology* 102, 139-150.
- Hindshaw, R.S., Tosca, N.J., Piotrowski, A.M., Tipper, E.T., 2018. Clay mineralogy, strontium and neodymium isotope ratios in the sediments of two High Arctic catchments (Svalbard). *Earth Surface Dynamics Discussions* 6.
- Hongxia, W., Xianjun, Z., Xianhong, L., Zhixun, Z., Zhenhong, L., Guangtao, Z., 2007. Geochemistry characteristics of sediment and provenance relations of sediments in core NT1 of the south Yellow Sea. *Journal of China University of Geosciences* 18, 287-298.
- Hong, Y.T., Hong, B., Lin, Q.H., Zhu, Y.X., Shibata, Y., Hirota, M., Uchida, M., Leng, X.T., Jiang, H.B., Xu, H., 2003. Correlation between Indian Ocean summer monsoon and North Atlantic climate during the Holocene. *Earth and Planetary Science Letters* 211, 371-380.
- Hu, B., Li, J., Zhao, J., Yan, H., Zou, L., Bai, F., Xu, F., Yin, X., Wei, G., 2018. Sr-Nd isotopic geochemistry of Holocene sediments from the South Yellow Sea: Implications for provenance and monsoon variability. *Chemical Geology* 479, 102-112.
- Ibarra, D.E., Caves, J.K., Moon, S., Thomas, D.L., Hartmann, J., Chamberlain, C.P., Maher, K., 2016. Differential weathering of basaltic and granitic catchments from concentration-discharge relationships. *Geochimica et Cosmochimica Acta* 190, 265-293.
- Jayananda, M., Moyen, J.F., Martin, H., Peucat, J.J., Auvray, B., Mahabaleswar, B., 2000. Late Archaean (2550-2520 Ma) juvenile magmatism in the Eastern Dharwar craton, southern India: constraints from geochronology, Nd-Sr isotopes and whole rock geochemistry. *Precambrian Research* 99, 225-254.

- Jiang, F., Xiong, Z., Frank, M., Yin, X., Li, A., 2019. The evolution and control of detrital sediment provenance in the middle and northern Okinawa Trough since the last deglaciation: Evidence from Sr and Nd isotopes. *Palaeogeography, Palaeoclimatology, Palaeoecology*.
- Jonell, T.N., Li, Y., Blusztajn, J., Giosan, L., Clift, P.D., 2018. Signal or noise? Isolating grain size effects on Nd and Sr isotope variability in Indus delta sediment provenance. *Chemical Geology* 485, 56-73.
- Joshi, R.K., Mazumdar, A., Peketi, A., Ramamurty, P.B., Naik, B.G., Kocherla, M., Carvalho, M.A., Mahalakshmi, P., Dewangan, P., Ramana, M.V., 2014. Gas hydrate destabilization and methane release events in the Krishna-Godavari basin, Bay of Bengal. *Marine and Petroleum Geology* 58, 476-489.
- Kessarkar, P.M., Rao, V.P., Ahmad, S.M., Patil, S.K., Kumar, A.A., Babu, G.A., Chakraborty, S., Rajan, R.S., 2005. Changing sedimentary environment during the Late Quaternary: Sedimentological and isotopic evidence from the distal Bengal Fan. *Deep Sea Research Part I: Oceanographic Research Papers* 52, 1591-1615.
- Kudrass, H., Hofmann, A., Dose, H., Emeis, K., Erlenkeuser, H., 2001. Modulation and amplification of climatic changes in the Northern Hemisphere by the Indian summer monsoon during the past 80 ky. *Geology* 29, 63-66.
- Kuksina, L.V., 2019. Suspended sediment yield and climate change in Kamchatka, Far East of Russia. *Proceedings of the International Association of Hydrological Sciences* 381, 55-64.
- Kulkarni, Y.R., Sangode, S.J., Bloemendal, J., Meshram, D.C., Suresh, N., 2015. Mineral magnetic characterization of the Godavari River and western Bay of Bengal sediments: Implications to source to sink relations. *Journal of the Geological Society of India* 85, 71-78.
- Lamy, F., Klump, J., Hebbeln, D., Wefer, G., 2000. Late Quaternary rapid climate change in northern Chile. *Terra Nova-Oxford* 12, 8-13.
- Li, J., Liu, S., Shi, X., Zhang, H., Fang, X., Chen, M.-T., Cao, P., Sun, X., Ye, W., Wu, K., 2018. Clay minerals and Sr-Nd isotopic composition of the Bay of Bengal sediments: Implications for sediment provenance and climate control since 40 ka. *Quaternary International* 493, 50-58.
- Lightfoot, P., Hawkesworth, C., 1988. Origin of Deccan Trap lavas: evidence from combined trace element and Sr-, Nd- and Pb-isotope studies. *Earth and Planetary Science Letters* 91, 89-104.
- Lightfoot, P.C., Hawkesworth, C.J., Devey, C.W., Rogers, N.W., Van Calsteren, P.W.C., 1990. Source and differentiation of Deccan Trap lavas: Implications of geochemical and mineral chemical variations. *Journal of Petrology* 31, 1165-1200.
- Lim, D., Jung, H., Choi, J., Yang, S., Ahn, K., 2006. Geochemical compositions of river and shelf sediments in the Yellow Sea: Grain-size normalization and sediment provenance. *Continental shelf research* 26, 15-24.
- Maccali, J., Hillaire-Marcel, C., Not, C., 2018. Radiogenic isotope (Nd, Pb, Sr) signatures of surface and sea ice-transported sediments from the Arctic Ocean under the present interglacial conditions. *Polar Research* 37, 1442982.

- Mahoney, J., Macdougall, J.D., Lugmair, G.W., Murali, A.V., Das, M.S., Gopalan, K., 1982. Origin of the Deccan Trap flows at Mahabaleshwar inferred from Nd and Sr isotopic and chemical evidence. *Earth and Planetary Science Letters* 60, 47-60.
- Mahoney, J.J., 1988. Deccan traps, Continental flood basalts. Springer, pp. 151-194.
- Mahoney, J.J., Sheth, H.C., Chandrasekharam, D., Peng, Z.X., 2000. Geochemistry of flood basalts of the Toranmal section, northern Deccan Traps, India: implications for regional Deccan stratigraphy. *Journal of Petrology* 41, 1099-1120.
- Mahowald, N.M., Muhs, D.R., Levis, S., Rasch, P.J., Yoshioka, M., Zender, C.S., Luo, C., 2006. Change in atmospheric mineral aerosols in response to climate: Last glacial period, preindustrial, modern, and doubled carbon dioxide climates. USGS Staff--Published Research, 166.
- Mazumdar, A., Dewangan, P., João, H.M., Peketi, A., Khosla, V., Kocherla, M., Badesab, F.K., Joshi, R.K., Roxanne, P., Ramamurty, P.B., 2009. Evidence of paleo-cold seep activity from the Bay of Bengal, offshore India. *Geochemistry Geophysics Geosystems* 10, Q06005.
- Mazumdar, A., Kocherla, M., Carvalho, M.A., Peketi, A., Joshi, R.K., Mahalaxmi, P., Joao, H.M., Jisha, R., 2015. Geochemical characterization of the Krishna-Godavari and Mahanadi offshore basin (Bay of Bengal) sediments: A comparative study of provenance. *Marine and Petroleum Geology* 60, 18-33.
- McCulloch, M.T., Wasserburg, G.J., 1978. Sm-Nd and Rb-Sr chronology of continental crust formation. *Science* 200, 1003-1011.
- Meyer, I., Davies, G.R., Stuut, J.B.W., 2011. Grain size control on Sr-Nd isotope provenance studies and impact on paleoclimate reconstructions: An example from deep-sea sediments offshore NW Africa. *Geochemistry, Geophysics, Geosystems* 12.
- Miriyala, P., Sukumaran, N.P., Nath, B.N., Ramamurty, P.B., Sijinkumar, A.V., Vijayagopal, B., Ramaswamy, V., Sebastian, T., 2017. Increased chemical weathering during the deglacial to mid-Holocene summer monsoon intensification. *Scientific reports* 7.
- Moyen, J.F., Martin, H., Jayananda, M., Auvray, B., 2003. Late Archaean granites: a typology based on the Dharwar Craton (India). *Precambrian Research* 127, 103-123.
- Melluso, L., Sethna, S.F., 2011. Mineral compositions in the Deccan igneous rocks of India: an overview, *Topics in igneous petrology*. Springer, pp. 135-159.
- Naidu, A.S., Mowatt, T.C., Somayajulu, B.L.K., Rao, K.S., 1985. Characteristics of clay minerals in the bed loads of major rivers of India. *MitteilungenausdemGeologische-PalaontologischenInstituts der Universitat Hamburg* 58, 559-568.
- Narkhedkar, S.G., Morwal, S.B., Padmakumari, B., Deshpande, C.G., Kothawale, D.R., Maheskumar, R.S., Kulkarni, J.R., 2015. Rainfall mechanism over the rain-shadow region of north peninsular India. *Climate Dynamics* 45, 1493-1512.
- Naqvi, S.M., Rogers, J.J.W., 1983. Precambrian of south India: Proceedings of the Indo-US workshop. Geological Society of India.

- Nesbitt, H., Young, G., 1982. Early Proterozoic climates and plate motions inferred from major element chemistry of lutites. *Nature* 299, 715-717.
- Pandey, B.K., Gupta, J.N., Sarma, K.J., Sastry, C.A., 1997. Sm-Nd, Pb-Pb and Rb-Sr geochronology and petrogenesis of the mafic dyke swarm of Mahbubnagar, South India: implications for Paleoproterozoic crustal evolution of the Eastern Dharwar Craton. *Precambrian Research* 84, 181-196.
- Past Interglacials Working Group of, P., 2016. Interglacials of the last 800,000 years. *Reviews of Geophysics* 54, 162-219.
- Parthasarathy, B., 1984. Interannual and long-term variability of Indian summer monsoon rainfall. *Proceedings of the Indian Academy of Sciences-Earth and Planetary Sciences* 93, 371-385.
- Pattan, J.N., Parthiban, G., PrakashBabu, C., Khadge, N.H., Paropkari, A.L., Kodagali, V.N., 2008. A note on geochemistry of surface sediments from Krishna-Godavari basin, East Coast of India. *J. Geol. Soc. India* 71, 107-114.
- Pattanayak, S.K., Shrivastava, J.P., 1999. Petrography and major-oxide geochemistry of Basalts from the eastern Deccan Volcanic province, India. In: Subbarao, K.V. (Ed.), *Deccan Volcanic province, West Volume, Mem. No. 43*, pp. 233-270., pp. 233-270.
- Peketi, A., 2013. Marine sedimentary Sulfur-Carbon-Iron systematics: A study from Krishna Godavari Basin, Bay of Bengal. *Andhra University*, p. 228.
- Peng, Z.X., Mahoney, J., Hooper, P., Harris, C., Beane, J., 1994. A role for lower continental crust in flood basalt genesis? Isotopic and incompatible element study of the lower six formations of the western Deccan Traps. *Geochimica et Cosmochimica Acta* 58, 267-288.
- Peucat, J., Vidal, P., Bernard-Griffiths, J., Condie, K., 1989. Sr, Nd, and Pb isotopic systematics in the archean low-to high-grade transition zone of Southern India: syn-accretion vs. post-accretion granulites. *The Journal of Geology*, 537-549.
- Perri, F., Critelli, S., Dominici, R., Muto, F., Tripodi, V., Ceramicola, S., 2012. Provenance and accommodation pathways of late Quaternary sediments in the deep-water northern Ionian Basin, southern Italy. *Sedimentary Geology* 280, 244-259.
- Pierson-Wickmann, A.-C., Reisberg, L., France-Lanord, C., Kudrass, H.R., 2001. Os-Sr-Nd results from sediments in the Bay of Bengal: Implications for sediment transport and the marine Os record. *Paleoceanography* 16, 435-444.
- Ponton, C., Giosan, L., Eglinton, T.I., Fuller, D.Q., Johnson, J.E., Kumar, P., Collett, T.S., 2012. Holocene aridification of India. *Geophysical Research Letters* 39, 1-6.
- Pradhan, S., Zhang, J., Baskaran, M., Shirodkar, P.V., Wu, Y., Pradhan, U.K., 2017. Investigations of the spatial and temporal variations of Sr and Nd isotopes in sediments from two Indian Rivers: Implications to source identification. *Geochemistry, Geophysics, Geosystems* 18, 1520-1536.
- Prasad, S., Anoop, A., Riedel, N., Sarkar, S., Menzel, P., Basavaiah, N., Krishnan, R., Fuller, D., Plessen, B., Gaye, B., 2014. Prolonged monsoon droughts and links to Indo-Pacific warm

pool: A Holocene record from Lonar Lake, central India. *Earth and Planetary Science Letters* 391, 171-182.

Radhakrishna, B.P., Naqvi, S.M., 1986. Precambrian continental crust of India and its evolution. *The Journal of Geology* 94, 145-166.

Raghunath, H.M., 2006. *Hydrology: principles, analysis and design*. New Age International.

Ramesh, R., Subramanian, V., Van Grieken, R., Van'tDack, L., 1989. The elemental chemistry of sediments in the Krishna river basin, India. *Chemical Geology* 74, 331-341.

Rao, V., 1991. Clay mineral distribution in the continental shelf sediments from Krishna to Ganges river mouth, east coast of India. *Indian journal of marine sciences* 20, 7-12.

Rao, G., 2001. Sedimentation, stratigraphy, and petroleum potential of Krishna-Godavari basin, East Coast of India. *AAPG bulletin* 85, 1623-1643.

Rashid, H., England, E., Thompson, L., Polyak, L., 2011. Late glacial to Holocene Indian summer monsoon variability based upon sediment. *Terr. Atmos. Ocean. Sci* 22, 215-228.

Roser, B.P., Korsch, R.J., 1988. Provenance signatures of sandstone-mudstone suites determined using discriminant function analysis of major-element data. *Chemical Geology* 67, 119-139.

Roy, A.B., Purohit, R., 2018. *Indian shield: Precambrian evolution and Phanerozoic reconstitution*. Elsevier.

Sijinkumar, A.V., Clemens, S., Nath, B.N., Prell, W., Benschila, R., Lengaigne, M., 2016. $\delta^{18}O$ and salinity variability from the Last Glacial Maximum to Recent in the Bay of Bengal and Andaman Sea. *Quaternary Science Reviews* 135, 79-91.

Singh, M., Singh, I.B., Muller, G., 2007. Sediment characteristics and transportation dynamics of the Ganga River. *Geomorphology* 86, 144-175.

Singh, S.K., Rai, S.K., Krishnaswami, S., 2008. Sr and Nd isotopes in river sediments from the Ganga Basin: Sediment provenance and spatial variability in physical erosion. *Journal of Geophysical Research: Earth Surface* 113, F03006, doi:10.1029/2007JF000909.

Singh, D.S., 2018. *The Indian Rivers: Scientific and Socio-economic Aspects*. Springer.

Silva, R., Mazumdar, A., Mapder, T., Peketi, A., Joshi, R.K., Shaji, A., Mahalakshmi, P., Sawant, B., Naik, B.G., Carvalho, M.A., 2017. Salinity stratification controlled productivity variation over 300 ky in the Bay of Bengal. *Scientific reports* 7, 14439.

Subramanian, V., 1996. The sediment load of Indian rivers-an update. *IAHS Publications-Series of Proceedings and Reports-Intern Assoc Hydrological Sciences* 236, 183-190.

Taylor, P., Chadwick, B., Moorbath, S., Ramakrishnan, M., Viswanatha, M., 1984. Petrography, chemistry and isotopic ages of Peninsular Gneiss, Dharwar acid volcanic rocks and the Chitradurga granite with special reference to the Late Archean evolution of the Karnataka craton, southern India. *Precambrian research* 23, 349-375.

- Tiwari, M., Ramesh, R., Somayajulu, B.L.K., Jull, A.J.T., Burr, G.S., 2005. Early deglacial (:19-17 ka) strengthening of the northeast monsoon. *Geophysical Research Letters* 32.
- Tripathy, G.R., Singh, S.K., Bhushan, R., Ramaswamy, V., 2011. Sr-Nd isotope composition of the Bay of Bengal sediments: Impact of climate on erosion in the Himalaya. *Geochemical Journal* 45, 175-186.
- Tutken, T., Eisenhauer, A., Wiegand, B., Hansen, B.T., 2002. Glacial-interglacial cycles in Sr and Nd isotopic composition of Arctic marine sediments triggered by the Svalbard/Barents Sea ice sheet. *Marine Geology* 182, 351-372.
- Vaithiyanathan, P., Ramanathan, A.L., Subramanian, V., 1988. Erosion, transport and deposition of sediments by the tropical rivers of India. IN: *Sediment Budgets*. IAHS Publication.
- Vimal, R., Banerjee, R., Gupta, S., Krishna, V., Achar, K.K., Babu, P.R., Parihar, P.S., Maithani, P.B., 2012. Geochemistry and Sr and Pb isotope systematics of basement granitoids from north and west of Palnad Sub-basin, Guntur and Nalgonda districts, Andhra Pradesh. *Jour. Appl. Geochem* 14, 295-315.
- Wasson, R.J., 2003. A sediment budget for the Ganga-Brahmaputra catchment. *Current Science*, 1041-1047.
- Wei, G., Liu, Y., Li, X., Shao, L., Liang, X., 2003. Climatic impact on Al, K, Sc and Ti in marine sediments: evidence from ODP site 1144, South China Sea. *GEOCHEMICAL JOURNAL-JAPAN-* 37, 593-602.
- Wei, G., Liu, Y., Li, X., Shao, L., Fang, D., 2004. Major and trace element variations of the sediments at ODP Site 1144, South China Sea, during the last 230 ka and their paleoclimate implications. *Palaeogeography, Palaeoclimatology, Palaeoecology* 212, 331-342.
- Wei, X., Wang, S., Ji, H., Shi, Z., 2018. Strontium isotopes reveal weathering processes in lateritic covers in southern China with implications for paleogeographic reconstructions. *PloS one* 13, e0191780.
- Windley, B.F., 1995. *The Evolving Continents*, John Wiley and Sons. 526p.
- Weltje, G.J., von Eynatten, H., 2004. Quantitative provenance analysis of sediments: review and outlook. *Sedimentary Geology* 171, 1-11.
- Wronkiewicz, D.J., Condie, K.C., 1987. Geochemistry of Archean shales from the Witwatersrand Supergroup, South Africa: source-area weathering and provenance. *Geochimica et Cosmochimica Acta* 51, 2401-2416.
- Young, G.M., Nesbitt, H.W., 1998. Processes controlling the distribution of Ti and Al in weathering profiles, siliciclastic sediments and sedimentary rocks. *Journal of Sedimentary Research* 68, 448-455.
- Zhou, Y., Xu, Y.J., Xiao, W., Wang, J., Huang, Y., Yang, H., 2017. Climate change impacts on flow and suspended sediment yield in headwaters of high-latitude regions-A case study in China's far northeast. *Water* 9, 966.

Figure and Table captions

Fig.1: Map showing lithology of Krishna and Godavari river drainage basins with sediment core locations (Red filled circle: MD161-8; Black filled circle: SK187/PC33). A= Deccan basalt (DcB) terrain, B=Proterozoic formations, C= Archean Proterozoic gneissic complex, D=Quaternary sediments. KDB= Krishna river drainage basin, GDB= Godavari river drainage basin.

Fig.2: Downcore profiles of MD161-8; (A) $^{87}\text{Sr}/^{86}\text{Sr}$ and ϵNd (B) Mg/Al ratio; (C) $\delta^{18}\text{O}_{\text{G.rubber}}$ profile from MD161-8 (Joshi et al., 2014); (D) Rb/Sr ratio; (E) Chemical Index of Alteration (CIA). Shaded regions denote marine isotope stages. Age scale of the studied core is based on Mazumdar et al. (2009) and Joshi et al. (2014). Black/red coloured arrow head indicates increment of corresponding parameter.

Fig.3: Sr and Nd isotope ratios mixing plot for the core MD161-8 (black open squares), SK187/PC33 (red open diamonds; Tripathy et al., 2011) along with isotopic ratios of different possible sediment sources (DcB: Deccan basalts; APGC: Archean Proterozoic Gneissic Complex; HH: Higher Himalayas; LH: Lower Himalayas). Average Sr and Nd concentrations and isotope ratios of the incorporated sediment sources are as follows, DcB (224.34 $\mu\text{g/g}$, 21.08 $\mu\text{g/g}$, 0.707113, -3.24), APGC (377.85 $\mu\text{g/g}$, 45.66 $\mu\text{g/g}$, 0.760536, -30.72), HH (80 $\mu\text{g/g}$, 18 $\mu\text{g/g}$, 0.76, -15) and LH (94 $\mu\text{g/g}$, 26 $\mu\text{g/g}$, 0.85, -24.4). Sr-Nd isotope ratios of river bed sediments of Krishna (red-colored plus symbols) and Godavari (black filled circles, black filled triangles) rivers are also incorporated (Ahmad et al., 2009 and this study).

Fig. 4: Temporal profiles of $^{87}\text{Sr}/^{86}\text{Sr}$ and clay contents (volume percentage; Joshi et al., 2014) of sediment core MD161-8

Table 1: Concentrations of Na, Mg, Al, K, Ca, Rb, Sr, Nd, Mg/Al, Rb/Sr, CIA and $^{87}\text{Sr}/^{86}\text{Sr}$ & ϵNd ratios of MD161-8.

Figure 1

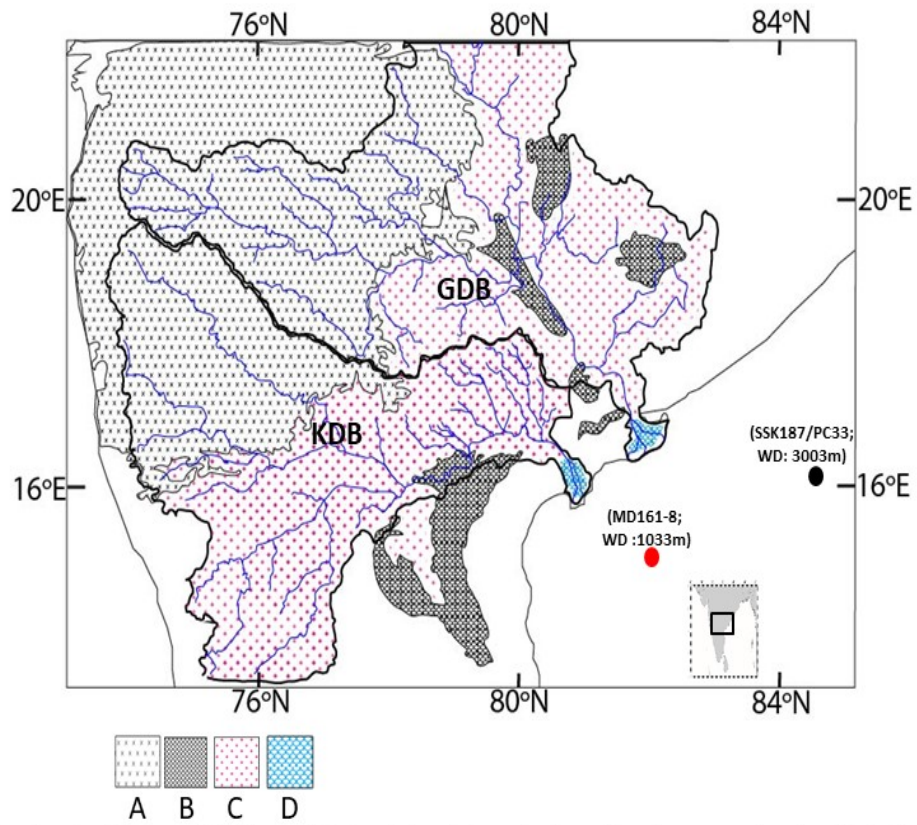


Fig. 1. Map showing lithology of Krishna and Godavari river drainage basins with sediment core locations (Red filled circle: MD161-8; Black filled circle: SSK187/PC33). A= Deccan basalts, B= Proterozoic formations, C= Archean gneissic complex, D= Quaternary sediments. KDB= Krishna river drainage basin, GDB= Godavari river drainage basin.

Figure 2

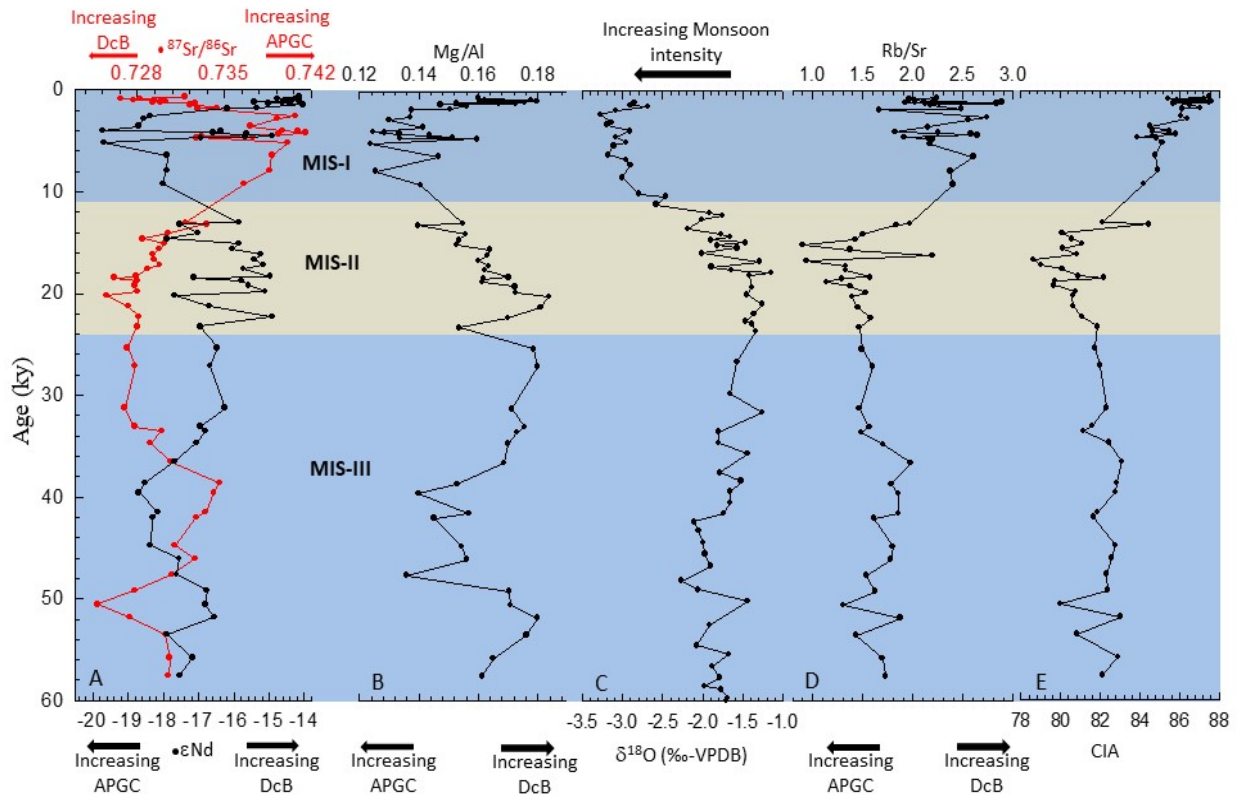


Fig. 2. Down core profiles of MD161-8. (A) $^{87}\text{Sr}/^{86}\text{Sr}$ and ϵNd . (B) Mg/Al ratio. (C) $\delta^{18}\text{O}_{\text{G.rubber}}$ profile from MD161-8 (Joshi et al., 2014). (D) Rb/Sr ratio. (E) Chemical Index of Alteration (CIA). Shaded regions denote marine isotope stages. Age scale of the studied core is based on Joshi et al. (2014). Arrow heads indicate increment of corresponding parameter.

Figure 3

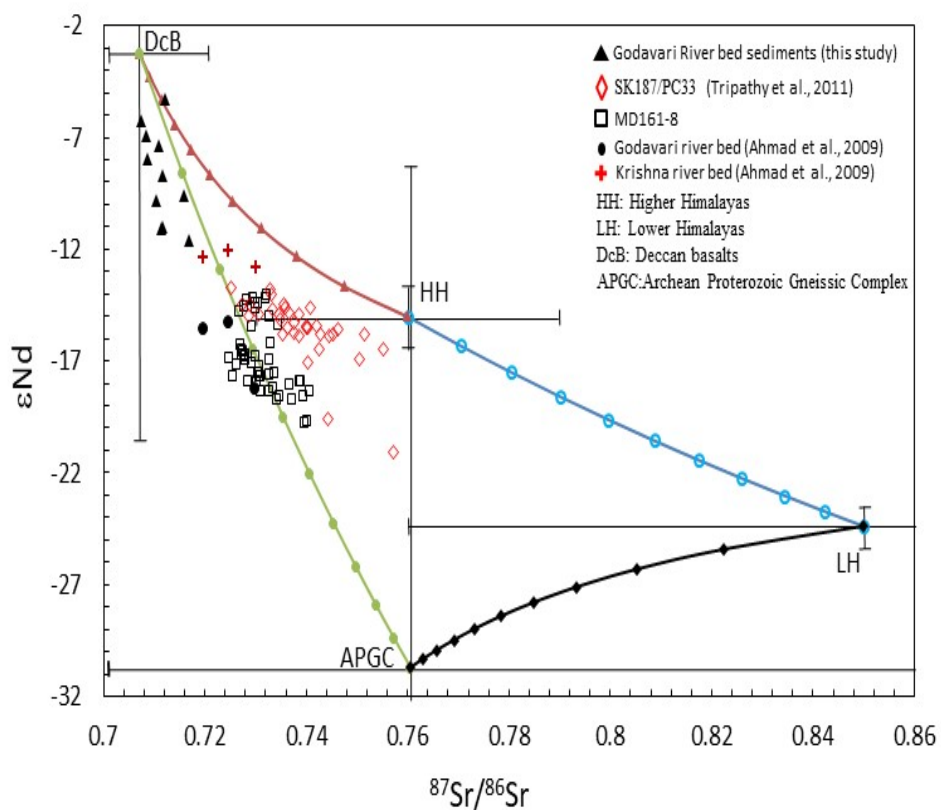


Fig. 3. Sr and Nd isotope ratios mixing plot for the core MD161-8 (black open squares), SK187/PC33 (red open diamonds; Tripathy et al., 2011) along with isotopic ratios of different possible sediment sources (DcB: Deccan basalts; APGC: Archean Proterozoic Gneissic Complex; HH: Higher Himalayas; LH: Lower Himalayas). Average Sr and Nd concentrations and isotope ratios of the incorporated sediment sources are as follows, DcB (224.34 $\mu\text{g/g}$, 21.08 $\mu\text{g/g}$, 0.707113, -3.24), APGC (377.85 $\mu\text{g/g}$, 45.66 $\mu\text{g/g}$, 0.760536, -30.72), HH (80 $\mu\text{g/g}$, 18 $\mu\text{g/g}$, 0.76, -15) and LH (94 $\mu\text{g/g}$, 26 $\mu\text{g/g}$, 0.85, -24.4). Sr-Nd isotope ratios of river bed sediments of Krishna (red-colored plus symbols) and Godavari (black filled circles, black filled triangles) rivers are also incorporated (Ahmad *et al.*, 2009 and this study).

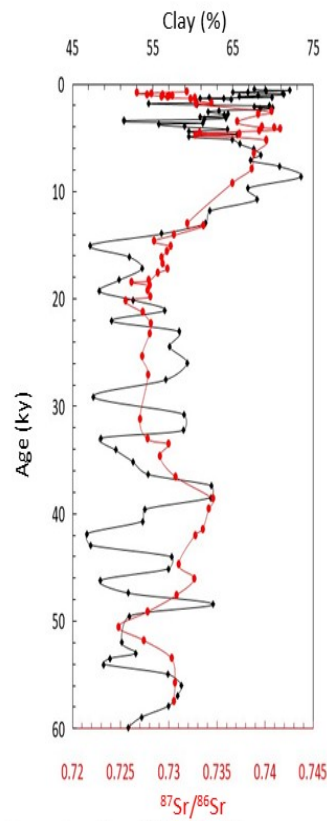


Fig. 4: Temporal profiles of $^{87}\text{Sr}/^{86}\text{Sr}$ and clay contents (volume percentage; Joshi et al., 2014) of sediment core MD161-8.

Figure 4

Table 1:

Sl. No	Age	Depth	Na	Mg	Al	K	Ca	Rb	Sr	Nd	Mg/Al	Rb/Sr	CIA	$^{87}\text{Sr}/^{86}\text{Sr}$	ϵNd
	(ky)	(mb sf)	(wt. %)	(wt. %)	(wt. %)	(wt. %)	(wt. %)	($\mu\text{g}/\text{gm}$)	($\mu\text{g}/\text{gm}$)	($\mu\text{g}/\text{gm}$)					
1	0.67	0.42	0.32	1.49	9.29	1.41	0.26	95.6	42.7	10.7	0.16	2.2	87.5	0.73183	-14.15
2	0.83	0.86	0.38	1.74	9.76	1.61	0.49	105.9	54.0	13.7	0.18	2.0	85.4	0.72666	-14.77
3	0.90	1.05	0.27	1.72	10.59	1.69	0.38	91.3	45.2	12.2	0.16	2.0	87.2	0.72818	-14.26
4	0.98	1.28	0.35	1.70	9.48	1.55	0.43	110.4	52.3	16.1	0.18	2.1	85.9	0.72770	-14.55
5	1.04	1.40	0.38	1.69	10.53	1.68	0.31	95.1	43.2	12.3	0.16	2.2	87.0	0.72932	-14.13
6	1.08	1.51	0.28	2.16	12.33	2.08	0.32	145.3	50.4	16.5	0.18	2.9	87.5	0.72998	-14.43
7	1.12	1.60	0.25	1.59	10.43	1.66	0.31	82.9	41.0	11.2	0.15	2.0	87.7	0.73031	-14.36
8	1.16	1.71	0.42	1.70	10.16	1.64	0.44	116.9	60.6	13.8	0.17	1.9	85.8	0.72920	-15.41
9	1.20	1.80	0.26	2.22	12.87	2.18	0.36	152.4	53.8	18.4	0.17	2.8	87.5	0.72990	-14.42
10	1.24	1.91	0.36	1.84	10.64	1.74	0.39	117.9	52.0	13.8	0.17	2.3	86.5	0.72984	-14.62
11	1.30	2.05	0.59	1.56	10.56	1.70	0.35	94.4	44.5	12.5	0.15	2.1	85.7	0.73267	-15.02
12	1.42	2.34	0.40	1.72	11.03	1.80	0.38	98.5	45.3	13.6	0.16	2.2	86.5	0.73225	-14.05
13	1.76	2.93	0.36	1.71	11.37	1.89	0.31	128.5	51.8	14.3	0.15	2.5	87.0	0.73443	-15.35
14	1.83	3.05	0.34	1.44	10.48	1.81	0.40	77.4	46.5	12.4	0.14	1.7	86.1	0.73282	-16.20
15	2.56	3.81	0.34	1.49	10.84	1.98	0.34	137.8	50.3	16.2	0.14	2.7	86.1	0.74066	-18.36
16	2.85	4.05	0.28	1.45	11.17	2.05	0.33	141.1	55.2	11.7	0.13	2.6	86.4	0.73928	-18.55
17	3.53	4.64	0.45	1.46	10.32	1.94	0.45	131.3	61.1	15.2	0.14	2.1	84.5	0.73707	-18.71
18	4.01	5.05	0.35	1.38	11.04	2.10	0.38	92.1	50.5	12.1	0.12	1.8	85.5	0.73966	-19.72
19	4.08	5.12	0.34	1.14	8.90	1.72	0.37	41.2	18.3	10.5	0.13	2.3	84.7	0.74094	-16.37
20	4.20	5.22	0.35	1.35	10.12	1.97	0.29	134.9	52.4	13.3	0.13	2.6	85.5	0.74155	-16.60
21	4.32	5.32	0.38	1.55	10.83	2.05	0.28	158.2	60.0	15.4	0.14	2.6	85.8	0.73939	-15.64
22	4.55	5.52	0.40	1.27	8.41	1.54	0.35	97.3	50.9	10.5	0.15	1.9	84.6	0.73317	-14.93

23	4.67	5.62	0.44	1.15	8.64	1.74	0.32	93.6	43.5	8.6	0.13	2.2	83.9	0.73733	-15.69
24	4.70	5.64	0.39	1.62	10.12	1.87	0.46	129.2	58.8	16.9	0.16	2.2	84.9	0.73273	-16.93
25	5.20	6.05	0.34	1.37	11.04	2.25	0.34	106.0	48.9	13.0	0.12	2.2	85.1	0.74011	-19.68
26	6.43	6.54	0.36	1.54	10.48	2.17	0.33	148.2	57.0	17.1	0.15	2.6	84.8	0.73881	-17.89
27	7.88	7.05	0.38	1.39	11.09	2.29	0.33	251.9	106.0	28.7	0.13	2.4	84.9	0.73859	-17.91
28	9.20	7.32	0.38	1.50	10.67	2.24	0.41	145.0	60.5	17.3	0.14	2.4	84.2	0.73659	-18.02
29	13.03	8.02	0.53	1.57	10.17	2.15	0.63	149.1	75.8	14.4	0.15	2.0	82.1	0.73187	-15.86
30	13.19	8.05	0.41	1.62	11.57	2.33	0.47	104.9	57.2	12.7	0.14	1.8	84.5	0.73359	-17.54
31	14.05	8.22	0.70	1.40	9.00	2.05	0.58	107.8	71.9	12.2	0.16	1.5	80.1	0.73050	-17.01
32	14.62	8.32	0.58	1.30	8.45	1.92	0.54	99.6	69.9	10.8	0.15	1.4	80.6	0.72842	-17.89
33	15.10	8.42	0.55	1.26	8.23	1.73	0.57	63.9	70.7	8.6	0.15	0.9	81.1	0.73019	-15.84
34	15.60	8.52	0.64	1.44	8.82	1.93	0.68	101.2	73.8	11.7	0.16	1.4	80.1	0.72979	-16.04
35	16.15	8.62	0.66	1.60	9.79	2.10	0.70	105.4	48.1	9.5	0.16	2.2	80.8	0.72921	-15.23
36	16.70	8.72	0.67	1.31	8.19	1.85	0.77	69.1	73.9	9.4	0.16	0.9	78.6	0.72936	-15.41
37	17.20	8.82	0.74	1.48	9.09	2.11	0.73	113.0	84.9	11.7	0.16	1.3	79.0	0.72982	-15.17
38	17.60	8.89	0.68	1.50	9.23	1.98	0.74	112.5	84.6	12.1	0.16	1.3	80.1	0.72881	-15.73
39	18.30	9.02	0.66	1.72	10.12	2.18	0.72	140.0	88.9	14.6	0.17	1.6	80.9	0.72790	-14.97
40	18.44	9.05	0.61	1.70	10.51	2.22	0.58	95.5	74.0	13.5	0.16	1.3	82.2	0.72612	-17.15
41	18.75	9.12	0.66	1.42	8.79	1.97	0.70	92.9	81.7	10.9	0.16	1.1	79.7	0.72802	-15.78
42	19.20	9.22	0.71	1.64	9.54	2.10	0.80	115.6	84.1	12.7	0.17	1.4	79.6	0.72777	-15.59
43	19.80	9.32	0.64	1.67	9.68	2.06	0.72	136.1	89.0	13.6	0.17	1.5	80.7	0.72804	-15.11
44	20.19	9.42	0.59	1.74	9.44	2.03	0.75	122.8	88.1	17.2	0.18	1.4	80.6	0.72549	-17.67
45	21.25	9.64	0.71	1.92	10.61	2.23	0.84	129.0	89.0	14.2	0.18	1.4	80.6	0.72726	-16.70
46	22.31	9.86	0.64	1.69	9.93	2.12	0.68	142.5	90.1	14.3	0.17	1.6	81.1	0.72813	-14.92
47	23.26	10.05	0.62	1.60	10.41	2.11	0.70	225.7	154.0	26.6	0.15	1.5	81.9	0.72799	-16.95
48	25.35	10.32	0.66	1.82	10.20	2.05	0.68	129.9	87.1	13.7	0.18	1.5	81.7	0.72722	-16.46
49	27.09	10.54	0.54	1.72	9.53	1.94	0.64	126.5	79.2	15.1	0.18	1.6	82.0	0.72784	-16.68
50	31.23	11.05	0.55	1.74	10.16	2.14	0.57	132.1	90.0	12.8	0.17	1.5	82.3	0.72700	-16.25
51	33.05	11.40	0.57	1.65	9.40	1.91	0.67	126.5	80.9	15.2	0.18	1.6	81.6	0.72780	-16.95

52	33.55	11.49	0.72	1.84	10.65	2.14	0.81	136.6	92.3	12.9	0.17	1.5	81.2	0.72994	-16.79
53	34.69	11.70	0.52	1.69	9.98	1.94	0.70	127.7	75.1	15.9	0.17	1.7	82.4	0.72907	-17.07
54	36.55	12.05	0.49	1.58	9.36	2.01	0.37	129.5	65.5	12.1	0.17	2.0	83.1	0.73068	-17.69
55	38.63	12.42	0.58	1.63	10.66	2.23	0.51	140.2	78.7	14.7	0.15	1.8	82.8	0.73458	-18.53
56	39.57	12.64	0.55	1.43	10.20	2.13	0.50	139.8	75.3	13.4	0.14	1.9	82.8	0.73415	-18.69
57	41.50	12.96	0.63	1.70	10.85	2.29	0.66	140.8	76.0	15.2	0.16	1.9	81.9	0.73351	-18.15
58	42.00	13.05	0.58	1.38	9.53	2.01	0.60	123.6	76.6	13.0	0.15	1.6	81.6	0.73272	-18.31
59	44.76	13.54	0.53	1.50	9.73	1.94	0.56	138.2	76.9	14.5	0.15	1.8	82.8	0.73103	-18.36
60	46.05	13.76	0.57	1.59	10.20	2.04	0.61	135.6	76.2	14.1	0.16	1.8	82.6	0.73265	-17.55
61	47.60	14.05	0.64	1.45	10.72	2.12	0.67	226.1	147.1	24.5	0.14	1.5	82.3	0.73079	-17.62
62	49.18	14.32	0.59	1.74	10.20	2.04	0.62	123.8	76.1	13.1	0.17	1.6	82.4	0.72776	-16.76
63	50.54	14.54	0.72	1.61	9.42	1.84	0.90	112.7	86.4	14.4	0.17	1.3	80.0	0.72477	-16.81
64	51.80	14.76	0.48	1.68	9.31	1.82	0.55	118.1	63.0	14.7	0.18	1.9	83.0	0.72738	-16.56
65	53.49	15.05	0.68	1.74	9.90	2.03	0.77	128.5	89.7	13.6	0.18	1.4	80.8	0.73027	-17.89
66	55.80	15.45	0.59	1.73	10.47	2.08	0.55	139.4	82.2	14.6	0.16	1.7	82.9	0.73063	-17.18
67	57.52	15.75	0.55	1.61	9.96	2.05	0.64	132.6	76.9	15.5	0.16	1.7	82.1	0.73050	-17.54

Supplementary material for Marine and Petroleum Geology

Monsoon rainfall and contrasting source rocks influenced sediment composition of peninsular basins along east coast of India (western Bay of Bengal)

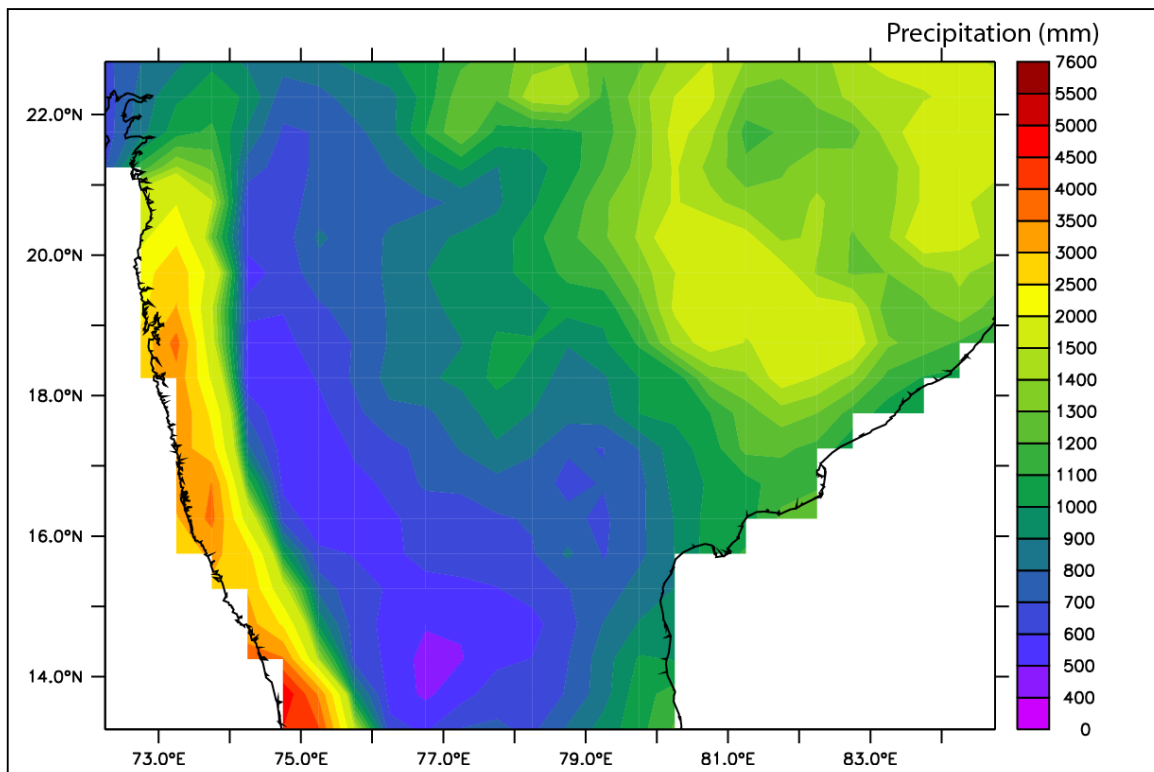
A. Peketi¹, A. Mazumdar¹, S.P.K. Pillutla¹, B. Sawant¹, V.K.Rai², A.V.S. Chaitanya¹, Ramakrsihnsna¹

¹CSIR- National Institute of Oceanography, Dona Paula, Goa-403004, India

² School of Earth and Space Exploration, Arizona State University, Tempe, AZ, 85287, USA

Corresponding Author: Aditya Peketi (aditya@nio.org)

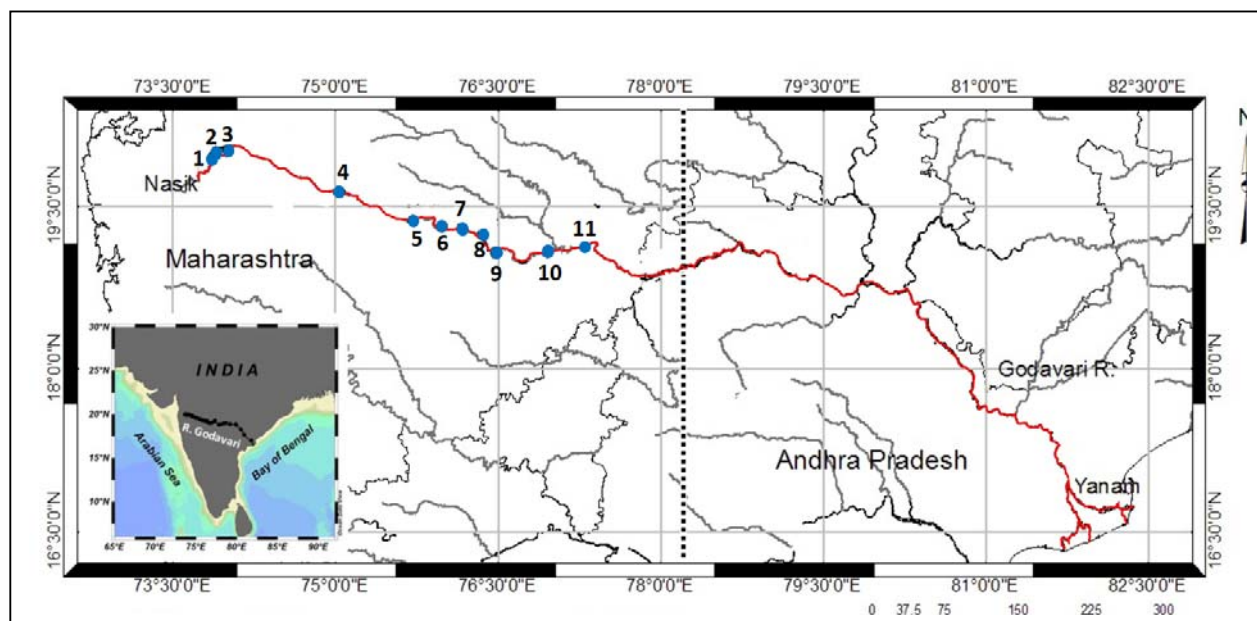
Suppl. Fig. F1. Annual precipitation (mm) for different meteorological sub-divisions of peninsular India based on data for the period 111 years (1901-2010)



Rainfall data for a period of 111 years (1901-2010) from the Krishna-Godavari drainage basin has been compiled. Annual cumulative rainfall over DcB and APGC terrains in the Krishna and Godavari river drainage basins for that time period was calculated based on the monthly rainfall data with a spatial coverage of 0.5-degree latitude x 0.5-degree longitude grid. The monthly rainfall data for the

corresponding time period were extracted from the Global Precipitation Climatology Project (GPCP) Version 6.0 (Becker et al., 2013; Schneider et al., 2014; ftp://ftp.dwd.de/pub/data/gpcc/html/fulldata_v6_doi_download.html). GPCP merges all available insitu worldwide rain gauge data at Global Precipitation climatology center (GPCC).

Supp. Fig.F2.Map showing Godavari river (red color) and river bed sampling locations, marked from 1 to 11 with blue filled circle.



Supp. Table 1: $^{87}\text{Sr}/^{86}\text{Sr}$ and ϵNd ratios of Krishna and Godavari river bed samples from river mouth. Data is from Ahmad et al. (2009).

Sr. No	Sample name	$^{87}\text{Sr}/^{86}\text{Sr}$	ϵNd
1	Krishna-1	0.73006	-12.78
2	Krishna-2	0.72173	-12.04
3	Krishna-3	0.72069	-12.33
4	Godavari-1	0.72998	-18.22
5	Godavari-2	0.72469	-15.31
6	Godavari-3	0.71963	-15.60

Supp. Table 2: $^{87}\text{Sr}/^{86}\text{Sr}$ and ϵNd ratios of Godavari river bed samples (this study).

Sr. No	Latitude (N)	Longitude (E)	$^{87}\text{Sr}/^{86}\text{Sr}$	ϵNd
1	20.01350	73.4375	0.71088	-7.39
2	20.00283	73.3783	0.71157	-8.74
3	19.59650	73.5433	0.71137	-11.12
4	19.33283	74.5547	0.70872	-7.97
5	19.21300	75.4305	0.71218	-5.32
6	19.16950	76.0972	0.71168	-11.04
7	19.08650	76.1263	0.70746	-6.24
8	19.13483	76.2185	0.71682	-11.59
9	19.04283	76.2885	0.70845	-6.89
10	19.04450	76.5763	0.71595	-9.56
11	19.17000	77.1702	0.71049	-9.83

References:

- Ahmad, S.M., Padmakumari, V.M., and Babu, G.A., 2009, Strontium and neodymium isotopic compositions in sediments from Godavari, Krishna and Pennar rivers: *Current science*, v. 97, p. 1766-1769, DOI:10.1029/2007JF000909.
- Becker, A., P. Finger, A. Meyer-Christoffer, B. Rudolf, K. Schamm, U. Schneider, and Ziese, M., 2013, A description of the global land-surface precipitation data products of the Global Precipitation Climatology Centre with sample applications including centennial (trend) analysis from 1901–present.: *Earth Syst. Sci. Data*, v. 5, p. 71-99, doi:10.5676/DWD_GPCC/CLIM_M_V2011_025.
- Schneider, U., Becker, A., Finger, P., Meyer-Christoffer, A., Ziese, M., and Rudolf, B., 2014, GPCC's new land surface precipitation climatology based on quality-controlled in situ data and its role in quantifying the global water cycle: *Theoretical and Applied Climatology*, v. 115, p. 15-40, DOI: 10.1007/s00704-013-0860-x.